Capturing the Thermal Radiation of Burning Diesel Sprays in a Pressurized Chamber

A. Pawlowski, R. Kneer*
Institute of Heat and Mass Transfer
RWTH Aachen University
Aachen, Germany

Abstract
In this study an infrared camera has been used to capture the radiation of a Diesel spray between 7.7 µm and 9.5 µm. This enabled the quantification of the thermal radiation emitted from the spray. The quantitative measurement of the radiation intensity allowed the determination of various spray properties by changing the background temperature. The experiments have been conducted at various ambient conditions up to 800 K and 5 MPa. At elevated ambient temperatures reflections from the chamber walls superposed with the radiation emitted from the spray. This prevents the quantification of the temperature of the liquid phase with this method for low effective spray emissivities.

Introduction

In Diesel engines the spray formation is known to have a strong impact on the performance of the engine. However, due to the extremely complex multi-phase flow, not all aspects of Diesel engine spray formation are fully understood yet. In order to enhance understanding, a vast number of experimental methods have been applied to this challenging spray process. Conventional methods like LDA or PDA [1] rely on visible light to determine the spray propagation. But also monochromatic x-rays have already been employed [2]. These methods usually aim to determine droplet velocities and diameters or mass distributions in the spray.

In order to characterize the fuel evaporation, also the fuel temperature is of interest. This has been successfully measured using UV-Raman-spectroscopy [3,4]. However, this particular method is restricted to molecules with OH-Bonds that are found e.g. in Ethanol. More recently multi-color-LIF has been employed [5], but this method appears to be difficult to apply to dense sprays at high temperatures. The fluorescence of Rhodamine B, a popular tracer for this purpose, reduces with temperature until it decomposes at 180°C.

So in this study an infrared camera is used to capture the radiation of the spray between 7.7 µm and 9.5 µm. This enabled the quantification of the thermal radiation originating from the spray. A radiation balance is sketched in Figure 1. Due to its temperature the spray emits radiation itself. However, the spray also transmits and reflects radiation. This is particularly relevant in an environment with walls much hotter than the spray like a combustion chamber.

The quantitative measurement of the radiation intensity allows the determination of various spray properties by changing the background temperature. The effective spray emissivity can be determined. For atmospheric ambient conditions the spray temperature can be measured. However, at Diesel engine conditions the large reflectivity of the spray prevents so far reliable temperature measurements.

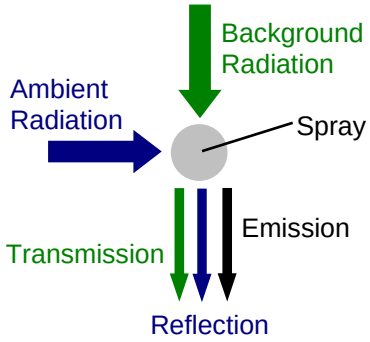

Figure 1: Sketch of radiation sources

Experimental Setup

Basic investigations have been conducted using a simple setup shown in Figure 2. The spray from an injector equipped with a single-orifice nozzle has been imaged in front of a background with a high emissivity ($\varepsilon \approx 1$). The temperature of this background is homogeneous and can be adjusted through a flow of water with controlled temperature.

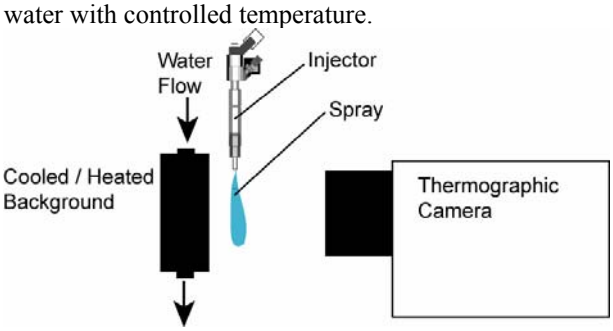

Figure 2: Sketch of the setup for atmospheric experiments

The infrared camera that has been used to capture the radiation of the spray is sensitive at wavelengths between 7.7 µm and 9.5 µm. Some results from these

* Corresponding author: kneer@wsa.rwth-aachen.de
Associated Web site: http://www.wsa.rwth-aachen.de
Proceedings of the 21th ILASS - Europe Meeting 2007

experiments are shown in the next section. For the atmospheric experiments the rail pressure was set to 40 MPa and the total energizing time was 1.45 ms to ensure quasi-steady condition. This is necessary, as the integration time of the camera is set to 50 µs to ensure sufficient photons on the detector.

A similar approach has then been used in the pressurized chamber. The spray is observed through an infrared-transmissive window made of BaF_2 (like in [6]) in a special window frame, opposite of which a cooled background is employed, see Figure 3. For the experiments in the pressurized chamber the rail pressure has been set to 80 MPa. The total energizing time is 1.5 ms and 75 µs have been chosen as the integration time of the camera.

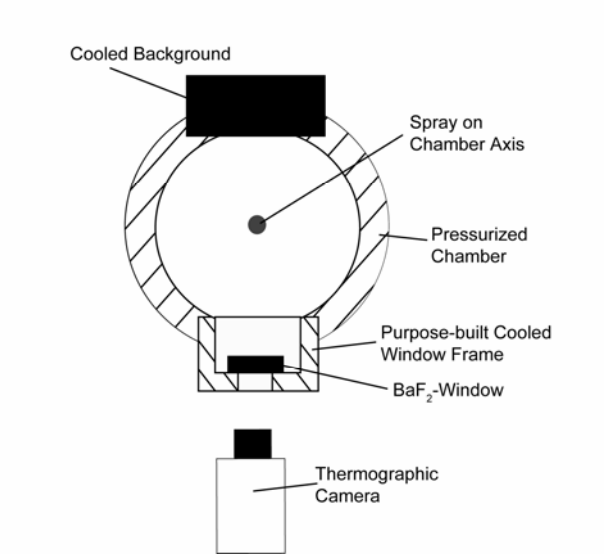

Figure 3: Cut through the pressurized chamber normal to spray and chamber axis

Atmospheric Results

Results 1.6 ms after the start of injector energizing for atmospheric conditions are shown in Figure 4 and Figure 5. Figure 4 shows the thermographic image for a temperature of the background of 323 K. The Diesel fuel jet appears as a cold region in front of a comparably hot background. Also the nozzle (upper part of the image) is colder than the background. Actually it is the part of the image with the lowest intensity. In Figure 5 the same configuration is shown for a cold background. The jet appears much warmer than the background, although its intensity is below what it is in the case with a hot background. This leads to the conclusion that the jet transmits some background radiation and its emissivity is therefore significantly smaller than 1. Note that in this experiment the highest intensity stems from the nozzle in the upper part of the image.

As the ambient temperature is low, reflectivity can be neglected. Assuming that the spray temperature is the same in both images, the radiation balance (Figure 1) for the intensity recorded by the camera can be written for the two background intensities as:

$$I_{Cam1} = \varepsilon_{Spray} I_{Spray,b} + (1-\varepsilon_{Spray}) I_{Background1} \quad (1)$$

$$I_{Cam2} = \varepsilon_{Spray} I_{Spray,b} + (1-\varepsilon_{Spray}) I_{Background2} \quad (2)$$

Subtracting equation (1) from (2) and solving for ε_{Spray} yields:

$$\varepsilon_{Spray} = 1 - \frac{I_{Cam2} - I_{Cam1}}{I_{Background2} - I_{Background1}} \quad (3)$$

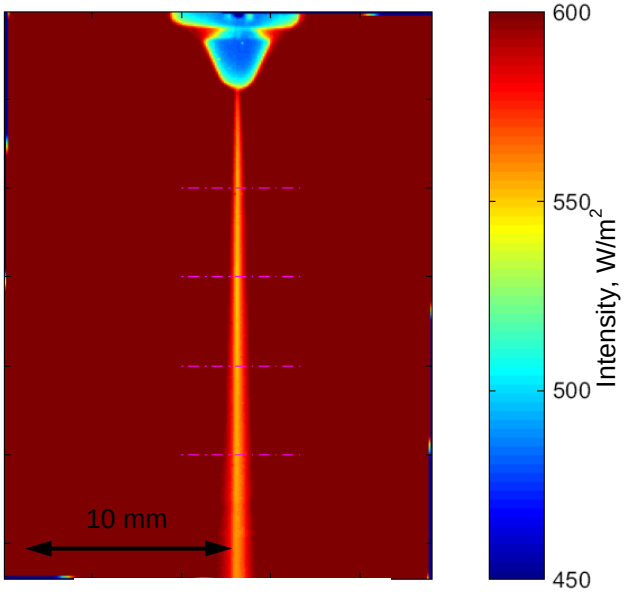

Figure 4: Recorded intensity distribution at a background temperature of 323 K

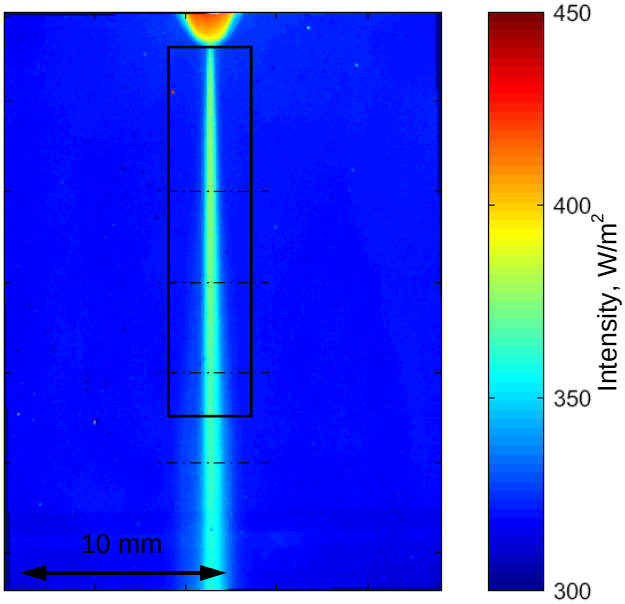

Figure 5: Recorded intensity distribution at a background temperature of 273 K – black rectangle indicates region of interest for the determination of emissivity and temperature

The result of this computation is shown in Figure 6. Please note that the aspect ratio in Figure 6 is 10:1 meaning that each recorded pixel is displayed 10 times

wider than high. This is due to the fact that under atmospheric conditions Diesel sprays are very narrow. The pixels representing the spray have been identified using a threshold. Outside the spray the emissivity has been set to unity. The spray shows the highest emissivities of around 0.3 on the axis and lower values towards the spray border.

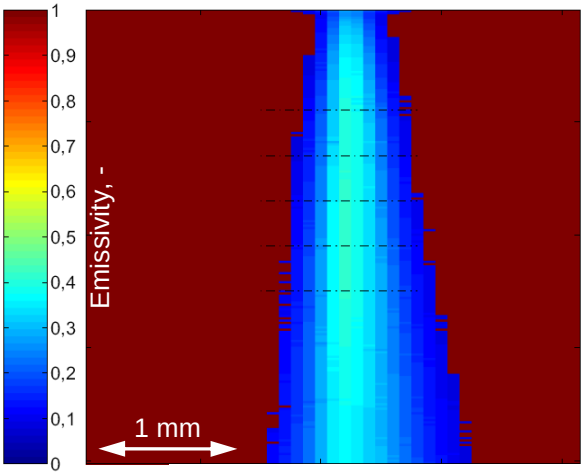

Figure 6: Computed emissivity distribution in the spray; image displayed with aspect ratio 10:1; see Figure 5 for definition of region of interest

Using the known emissivity of the spray, its temperature can be determined from the intensity distribution using the Stefan-Boltzmann-Law. The result is shown in Figure 7. The spray exhibits a comparably uniform temperature distribution around 305 K. Please note that for better clarity this image also is shown with an aspect ratio of 10:1.

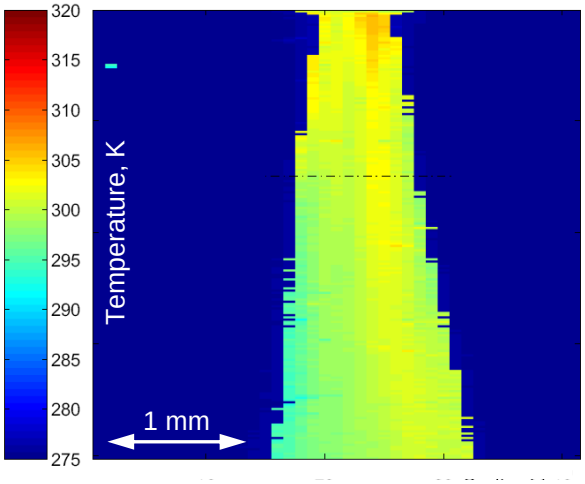

Figure 7: Computed temperature distribution in the spray; image displayed with aspect ratio 10:1; see Figure 5 for definition of region of interest

Results in the Pressurized Chamber

The left image in

Figure 8 is taken under atmospheric conditions at an ambient density of 1.2 kg/m^3. The other images in Figure 8 have been taken in the pressurized chamber at an ambient density around 21 kg/m^3, and different ambient temperatures and pressures. See Figure 3 for a sketch of the experimental setup. All images have been taken at 1.5 ms after the start of the energizing time of the injector at a rail pressure of 80 MPa. The total energizing time is 1.5 ms and 75 µs have been chosen as the integration time of the camera.

The higher ambient density in the right four images in

Figure 8 leads to a much wider spray angle compared to the atmospheric case. This can be seen particularly well in the case with ambient conditions of 500 K and 3.2 MPa, where evaporation is comparably slow and therefore the spray can be seen better than in the hotter conditions. Only the liquid phase is expected to emit or reflect thermal radiation whereas at these temperatures the radiation from the gas is supposed to be negligible. At higher ambient temperatures the spray cone angle remains the same; however the spray evaporates and therefore the observed liquid penetration length reduces. Thermal radiation from burning fuel can be seen in the image taken at ambient conditions of 800 K and 5 MPa.

Figure 9 shows images of the Diesel spray at different times after the start of the energizing of the injector. The ambient temperature is 700 K and the ambient pressure is 4.2 MPa. The liquid phase image changes only little between 500 µs and 2000 µs, so the assumption of quasi-steady conditions is justified.

Figure 10 shows a similar series of images for ambient conditions of 5 MPa and 800 K. Due to the higher ambient temperature the liquid spray penetration reduces significantly. However, the images taken 1500 µs and 2000 µs after the start of the energizing time of the injector indicate clearly radiation from burning fuel. The radiation from the liquid shows only little variation, justifying again the assumption of quasi-steady conditions for the liquid phase.

Like in atmospheric conditions the determination of the spray temperature has been attempted. However no reasonable result could be achieved. This is probably due to the high reflectivity of the spray. From a variation of the background temperature the spray transmissivity could be determined, assuming that the radiation reflected and emitted by the spray are independent on the background temperature. From two images at ambient conditions of 500 K and 3.2 MPa with background temperatures of 288 K and 323 K and an operation similar to that outlined in equation (1) to (3) the spray transmissivity has been determined. The result is shown in Figure 11. On the spray centerline the transmissivity is only about 0.1, increasing towards the spray border. Assuming a similar spray emissivity like in the atmospheric case of around 0.3, it is probably the spray reflectivity that dominates the total recorded radiation.

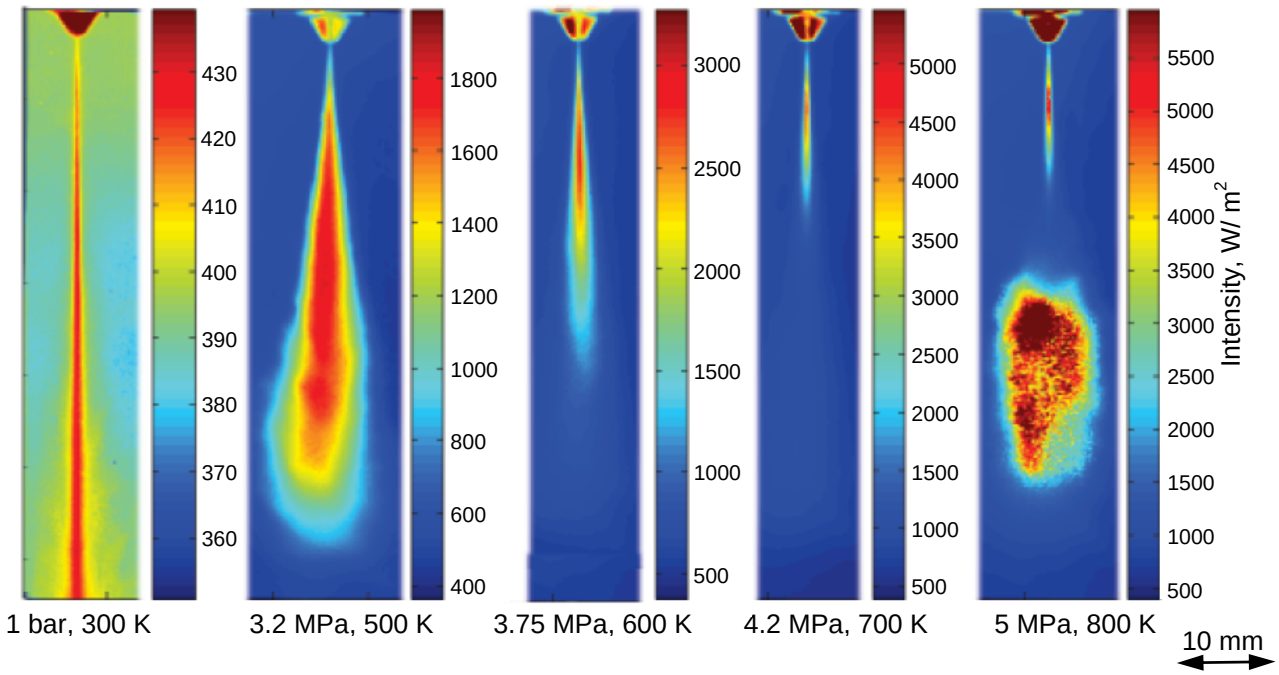

Figure 8: Thermographic spray images under different ambient conditions, all at 80 MPa rail pressure and 1.5 ms after the start of the energizing time of the injector

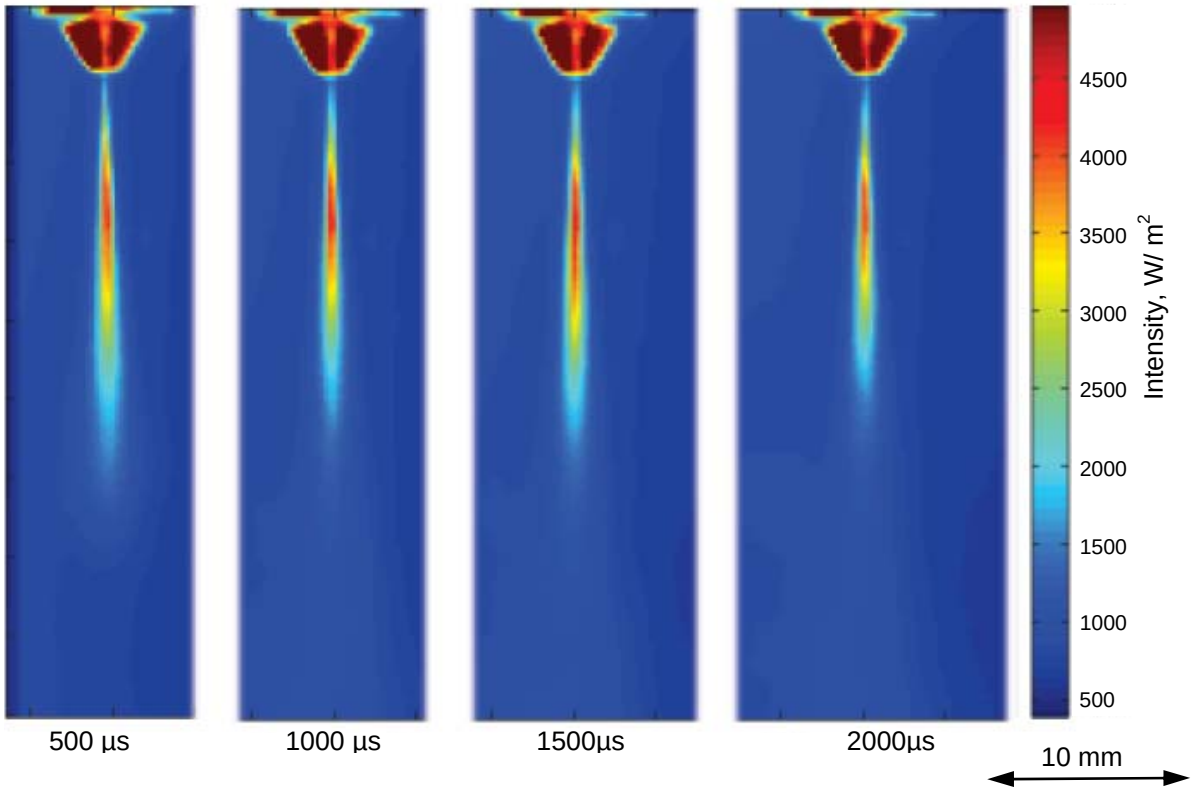

Figure 9: Thermographic spray images at different times after the start of the energizing time of the injector, all at 80 MPa rail and at 4.2 MPa ambient pressure and 700 K ambient temperature

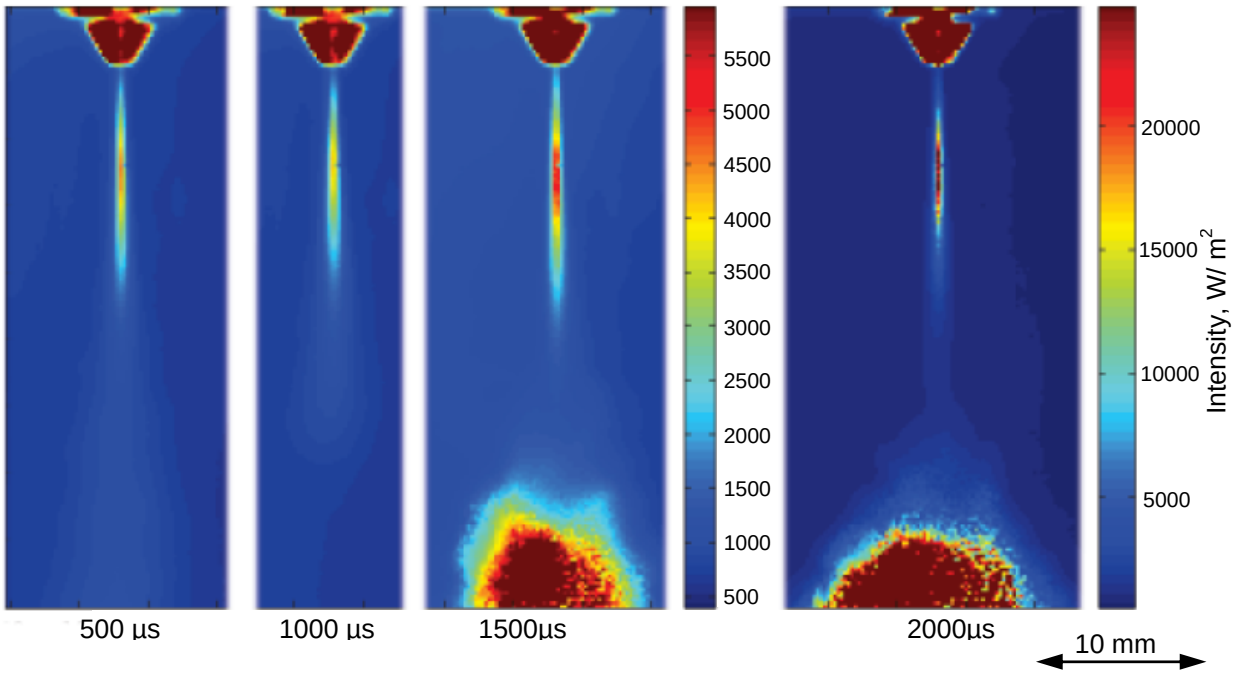

Figure 10: Thermographic spray images at different times after the start of the energizing time of the injector, all at 80 MPa rail and at 5 MPa ambient pressure and 800 K ambient temperature

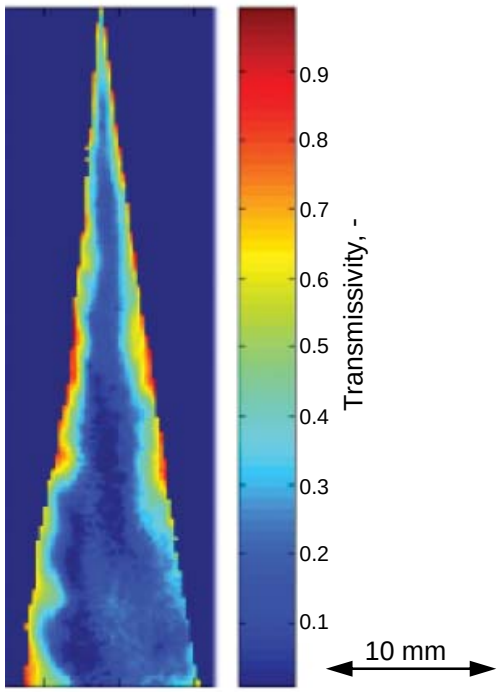

Figure 11: Transmissivity distribution in the spray at ambient conditions of 500 K and 3.2 MP

Development of a Heatable Liner

So one principal problem in determining the spray temperature in the pressurized chamber is that two different sources irradiate on the spray: the hot inner chamber walls and the cold background. In order to overcome the restriction only to be able to vary the temperature of the background, but not of the rest of the chamber interior, a heatable inner liner has been developed for the pressurized chamber. It allows controlling uniformly the temperature of the chamber inner wall. This allows combining the transmission and the reflection terms in the spray radiation balance, cf. Figure 1. Such a procedure allows determining the spray temperature using a treatment very similar to that outlined in equation (1) to (3), where reflectivity has been neglected.

A heatable inner liner satisfying the requirements has been constructed and tested under atmospheric conditions. However in order to limit heat losses in the test section only heating and no cooling capacity has been foreseen. Therefore in the atmospheric tests, the background and ambient temperature has been significantly higher than the fuel temperature, as will be the case for tests in the pressurized chamber. One representative configuration is a spray temperature around 300 K and background temperatures of T_{Back1} = 358 K and T_{Back2} = 400 K.

Determining the spray temperature from these measurements resulted in some difficulties prohibiting measurements in the chamber, as solving for the spray temperature is physically possible but can be badly conditioned depending on spray and background parameters. When the ambient temperature is varied uniformly, the equations (1) to (3) hold again. Resubstituting equation (3) into equation (1), using the Stefan-Boltzmann-law and solving for the spray temperature gives:

$$T_{Spray} = \left(\frac{T_{Cam1}^4 - \frac{\left(T_{Cam1}^4 - T_{Cam2}^4\right) T_{Back1}^4}{T_{Back1}^4 - T_{Back2}^4}}{1 - \frac{T_{Cam1}^4 - T_{Cam2}^4}{T_{Back1}^4 - T_{Back2}^4}} \right)^{1/4} \quad (4)$$

In order to determine the sensitivity to measurement errors in e.g. the temperature recorded by the infrared camera T_{Cam1} at background temperature T_{Back1} one needs to take the derivative of equation (4) with respect to T_{Cam1}. Doing so and evaluating the resulting expression with the measured data gives a value of dT_{Spray}/dT_{Cam1} of 12. This means 1 K measurement inaccuracy in the determination of T_{Cam1} results inevitably in 12 K inaccuracy of the spray temperature. This result is based on an effective spray emissivity of 0.25. The error depends strongly on this parameter, see Figure 12:

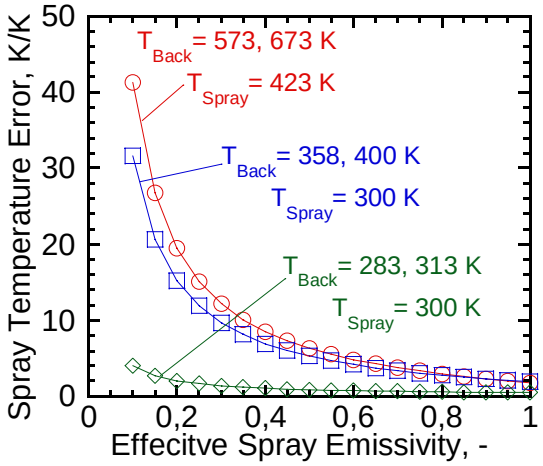

Figure 12: Sensitivity to measurement inaccuracies depending on spray emissivity for different ambient conditions

Figure 12 is based on calculations, where spray temperature and effective emissivity are assumed, together with the background temperatures. These parameters allow the computation of the temperatures recorded by the camera. Generally the measurement accuracy improves dramatically with increasing emissivity. So one possibility to perform measurements in the chamber is to employ a dye that increases the effective spray emissivity.

However, Figure 12 also shows that the chosen atmospheric conditions with T_{Back} = 358 and 400 K represent well the difficulties that need to be encountered at the pressurized chamber. For this case, assuming a spray temperature of 423 K and beckground temperatures of T_{Back} = 573 and 673 K, similar sensitivities occur than in the case, that was tested under atmospheric conditions. In case of background temperatures below and above the spray temperature (T_{Back} = 300 K, T_{Back} = 283 and 313 K), only a very small sensitivity is observed. However, employing such conditions in a pressurized chamber, which simulates conditions relevant for Diesel injection processes, is probably infeasible.

Conclusions

Diesel injection processes have been observed using a thermographic camera. The thermal radiation from these injections has been captured under atmospheric conditions as well as under conditions relevant for Diesel engines, at 5 MPa and 800 K. This enabled capturing not only the thermal radiation of the liquid spray but also the one of the flame.

The temperature of the liquid fuel has been determined under atmospheric conditions. Strong reflections of the chamber walls prevented the temperature measurement under "hot" conditions. This problem could not be solved with a heatable inner liner for the chamber, because then the measurements become extremely sensitive to measurement inaccuracies. However, the authors are confident that this issue can be overcome by increasing the effective emissivity of the spray.

Acknowledgements

This work was financially supported by General Motors Company, R&D. The authors also want to thank Dr. Michael Staudt for his ideas and his early work on this topic, as well as our student co-workers Tim Lowak, Karola Sommer and Heike Schreiber.

References

1. Albrecht, H.; Borys, M.; Damaschke, N., Tropea, C., "Laser Doppler and Phase Doppler Measurement Techniques" Springer-Verlag Berlin Heidelberg New York, 2003
2. Yue, Y., Powell, C. F., Poola, R., Wang, J., Schaller, J.K., "Quantitative Measurements of Diesel Fuel Spray Characteristics in the Near-Nozzle Region using X-Ray Absorbtion", Atomization and Sprays, vol. 11, pp. 479-490, 2001
3. Beushausen, V., Mueller, T., Hentschel. W., "2D Characterization of Alcohol Sprays by Means of 1D Spontaneous Raman Scattering", ILASS-Europe, Darmstadt, Germany, 2000
4. Weber, J., Spiekermann, P., Peters, N., "Comparison of Experimental Investigation and Numerical Simulation of a High Pressure Fuel Spray", ICLASS, Kyoto, Japan, 2006
5. Lavieille, P., Delconte, A., Blondel, D., Lebouché, M., Lemoine, F., "Non-intrusive temperature measurements using three-color laser-induced flourescence", Experiments in Fluids, 36, pp. 706-716, 2004
6. Labs, J., Parker, T. , "Two-dimensional droplet size and volume fraction distributions from the near-injector region of high-pressure Diesel sprays", Atomization and Sprays, vol. 16, pp. 843-855, 2006